BRAIN
ORIGINAL ARTICLE

Thalamic epileptic spikes disrupt sleep spindles in patients with epileptic encephalopathy

Anirudh Wodeyar,[1,2,3] Dhinakaran Chinappen,[2,4] Dimitris Mylonas,[5,6] Bryan Baxter,[5,6] Dara S. Manoach,[5,6] Uri T. Eden,[1,7] Mark A. Kramer[1,7,†] and Catherine J. Chu[2,3,†]

[†]These authors contributed equally to this work.

In severe epileptic encephalopathies, epileptic activity contributes to progressive cognitive dysfunction. Epileptic encephalopathies share the trait of spike-wave activation during non-REM sleep (EE-SWAS), a sleep stage dominated by sleep spindles, which are brain oscillations known to coordinate offline memory consolidation. Epileptic activity has been proposed to hijack the circuits driving these thalamocortical oscillations, thereby contributing to cognitive impairment.

Using a unique dataset of simultaneous human thalamic and cortical recordings in subjects with and without EE-SWAS, we provide evidence for epileptic spike interference of thalamic sleep spindle production in patients with EE-SWAS.

First, we show that epileptic spikes and sleep spindles are both predicted by slow oscillations during stage two sleep (N2), but at different phases of the slow oscillation. Next, we demonstrate that sleep-activated cortical epileptic spikes propagate to the thalamus (thalamic spike rate increases after a cortical spike, $P \approx 0$). We then show that epileptic spikes in the thalamus increase the thalamic spindle refractory period ($P \approx 0$). Finally, we show that in three patients with EE-SWAS, there is a downregulation of sleep spindles for 30 s after each thalamic spike ($P < 0.01$).

These direct human thalamocortical observations support a proposed mechanism for epileptiform activity to impact cognitive function, wherein epileptic spikes inhibit thalamic sleep spindles in epileptic encephalopathy with spike and wave activation during sleep.

1 Department of Mathematics and Statistics, Boston University, Boston, MA 02215, USA
2 Department of Neurology, Massachusetts General Hospital, Boston, MA 02114, USA
3 Harvard Medical School, Boston, MA 02115, USA
4 Graduate Program in Neuroscience, Boston University, Boston, MA 02215, USA
5 Department of Psychiatry, Massachusetts General Hospital, Boston, MA 02215, USA
6 Division of Sleep Medicine, Harvard Medical School, Boston, MA 02115, USA
7 Center for Systems Neuroscience, Boston University, Boston, MA 02215, USA

Correspondence to: Catherine Chu, MD
Department of Neurology, Massachusetts General Hospital
100 Cambridge Street, Suite 2036, Boston, MA 02114, USA
E-mail: cjchu@mgh.harvard.edu

Keywords: EE-SWAS; cross-frequency relationships; interictal discharges; non-rapid eye movement sleep; memory consolidation

Received September 18, 2023. Revised March 01, 2024. Accepted March 24, 2024. Advance access publication April 23, 2024

Introduction

Cognitive dysfunction is a common comorbidity in epilepsy,[1-3] but the mechanism remains unknown.[4] In the most severe form, cognitive dysfunction is described as an epileptic encephalopathy (EE), in which patients have a reduced rate of development, plateau or frank regression in cognitive functions concurrent with the development of epileptiform activity.[5] Several epileptic encephalopathies share the trait of interictal epileptic spikes that are potentiated during non-REM sleep, termed epileptic encephalopathy associated with spike-wave activation during sleep (EE-SWAS). In these cases, epileptic spikes during sleep are thought to be related mechanistically to cognitive decline[6]; however, direct measures of epileptic spike rates in sleep fail to predict cognitive symptoms in EE-SWAS.[7-10]

Non-REM stage two (N2) sleep is characterized electrophysiologically by the presence of sleep spindles, which are prominent bursts of 9–15 Hz oscillations. Sleep spindles originate in the thalamus and propagate to the cortex and occur with an approximate period of 2–5 s, dictated by an after-depolarization spindle refractory period.[11,12] Spindles are frequently nested in the up-state of slow oscillations (0.5–2 Hz oscillations)[13-15] and, critically, spindle rate is correlated with cognitive measures.[16,17] Sleep spindles are implicated specifically in supporting sleep-dependent memory consolidation,[18-20] at least in part through coordination of hippocampal ripples.[20-22]

Epileptic spikes, in contrast to sleep spindles, are cortically driven pathological events, reflecting summated, excessively synchronous neural activity.[23,24] Observations in animals[25] and in humans[26,27] demonstrate that cortical epileptic spike activity may propagate to the thalamus.[28] Epileptic spikes have been proposed to hijack the thalamocortical circuitry that produces sleep spindles and thereby disrupt sleep-dependent memory consolidation,[4] with several studies observing a negative correlation between spikes and spindles.[29-33] However, how and whether cortical spikes interact and interfere with thalamic activity to disrupt thalamocortical sleep spindles in humans remains unknown. Direct observations of these dynamics are challenging owing to the rare condition of EE-SWAS and the scarcity of recordings available from the human thalamus.

Using a unique dataset of simultaneous human thalamic and cortical recordings in subjects with and without EE-SWAS, we provide direct evidence for epileptic spike interference of thalamic sleep spindle production in EE-SWAS. We find that cortical slow oscillations predict both epileptic spikes and spindles during N2 sleep at different phases of the slow oscillation. We also show that sleep-activated cortical epileptic spikes are more likely to propagate to the thalamus than spike populations that are not sleep activated. Finally, we demonstrate that thalamic spikes inhibit spindle production, most prominently in subjects with EE-SWAS. Taken together, this work provides *in vivo* human evidence that epileptic spikes are both supported by and disrupt thalamocortical oscillations present during sleep. Furthermore, sleep spindles are most disrupted in patients with EE-SWAS, supporting this interference as a plausible mechanism contributing to cognitive dysfunction in these patients.

Materials and methods

Subject data collection

Consecutive subjects with simultaneous thalamic and cortical local field potentials and scalp EEG recording collected as part of their clinical evaluation for drug-resistant epilepsy at Massachusetts General Hospital were evaluated. Informed consent was received from all patients included in this study. To ensure appropriate thalamic sampling relative to the cortical irritative zone, only those subjects found to have instantaneous ictal cortical propagation to the thalamic target were included, resulting in datasets from nine subjects. In these subjects, thalamic leads targeted the centromedian nucleus in seven subjects and the anterior nucleus in two subjects. Clinical diagnosis, the location of the seizure onset zone, antiseizure medications and demographic information were collected from chart review (Table 1). Pre- and postoperative high-resolution MRIs were collected for electrode co-registration. This study was approved by the Massachusetts General Hospital Institutional Review Board.

EEG data collection, preprocessing and channel selection

Intracranial and scalp EEG data were collected using the clinical Natus Quantum system (Natus Neurology Inc.). Depth electrodes (PMT Depthalon depth platinum electrodes with 3.5 mm spacing, 2 mm contacts and 0.8 mm diameter; or Ad-tech depth platinum electrodes with 5–8 mm spacing, 2.41 mm contact size and 1.12 mm diameter) were placed in the regions of clinical interest and sampled at 1024 Hz (eight subjects) or 2048 Hz (one subject, subsequently downsampled to 1024 Hz). Twenty-four hours of scalp EEG data (21 scalp electrodes plus ECG and electroculogram electrodes) were sleep-staged by a board-certified clinical neurophysiologist

Table 1 Subject characteristics

ID	Sex	Aetiology	N2 duration (h)	ASM	Thalamic target	Cortical target	SWAS	EE
1	Male	Stroke	4.98	CBD, LTG, CLB	CM	Parietal	No	No
2	Male	Non-lesional	7.95	CLB, LTG	AN	Temporal	No	No
3	Male	Non-lesional	3.67	OXC, TOP, LTG	AN	Frontal	No	No
4	Male	Malformation of cortical development	5.54	TOP, LTG, LEV	CM	Parietal	Yes	No
5	Female	Non-lesional	7.32	LAC, PER, ZON, CZP	CM	Frontal	Yes	No
6	Male	Non-lesional	3.56	CLB, LEV	CM	Frontal	Yes	No
7	Male	Non-lesional	8.34	LEV, VPA, LTG	CM	Frontal	Yes	CSWS
8	Male	Malformation of cortical development	6.69	LTG, RFM, ESL, CZP, LOR	CM	Frontal	Yes	LGS
9	Female	Encephalitis	5.85	LEV, LTG, CLB	CM	Frontal	Yes	LGS

AN = anterior nucleus; ASM = anti-seizure medications; carbamazepine; CBD. cannibidiol; CLB = clobazam; CM = centromedian nucleus; CSWS = continuous spike and wave of sleep with encephalopathy; CZP; EE = clinical epileptic encephalopathy diagnosis; ESL = eslicarbazepine; LAC = lacosamide; LGS = Lennox Gastaut syndrome; LOR = lorazepam; LTG = lamotrigine; N2 = stage two non-REM sleep; OXC = oxcarbazepine = TOP = topiramate = LEV = levetiracetam; PER = perampanel; RFM = rufinamide; SWAS = spike-wave activation during sleep; VPA = valproic acid; ZON = zonisamide.

(C.J.C.) following standard visual criteria.[34,35] To control for variability across sleep stages and focus on sleep-activated epileptic spike activity and sleep spindles, we selected only non-REM stage two sleep segments (N2) for analysis. All N2 sleep segments over the course of the 24 h interval were concatenated for analysis.

For epileptic spike and spindle detections, we evaluated three voltage time series from each subject: (i) adjacent thalamic depth electrode contacts with the highest-amplitude signal in a bipolar reference; (ii) adjacent cortical depth electrode contacts in the clinically determined seizure onset zone in a bipolar reference; and (iii) scalp EEG in a bipolar reference CZ–PZ. To detect slow oscillations, we analysed the scalp CZ contact using a midline, far-field non-cephalic reference placed over the second cortical spinous process.[14,22] We applied bipolar referencing for improved spatial resolution. The channel and reference used to test each hypothesis are stated in the 'Results' section.

Automatic event detection

Epileptic spike detection

To detect epileptic spikes, we extended a previously developed method.[36,37] First, we bandpass filtered the data both forwards and backwards using a finite impulse response (FIR) filter between 25 and 80 Hz (MATLAB function *firfilt*). We then applied a Hilbert transform and calculated the analytic signal and the amplitude envelope of this signal. For each voltage signal, the moments when the amplitude envelope exceeded three times the mean amplitude were identified as candidate spikes. To ensure the candidate spikes were not attributable to gamma-band oscillatory bursts, we also calculated the regularity of oscillations in an interval (±0.25 s) around each candidate spike. To assess the regularity of the signal in this interval, we computed the Fano factor,[38] estimated by: (i) detrending the interval of unfiltered data at each candidate spike; (ii) identifying peaks and troughs; (iii) calculating the inter-peak and inter-trough intervals; and (iv) estimating the ratio of the variance of the inter-peak and inter-trough intervals to the mean of the inter-peak and inter-trough intervals. We then removed candidate spikes if the maximum amplitude (calculated by rectifying the data and identifying the maximum voltage) of the unfiltered data at the candidate spike was below three times the mean amplitude or if the Fano factor was <2.5; we note that Fano factors below one indicate a more regular rhythm, with zero indicating no variability in the inter-peak or inter-trough intervals. Of the resulting spikes, those detected within 20 ms of one another were merged into a single spike detection. We visually examined individual detections and the averaged spike waveform to confirm that the method accurately detected epileptic spikes in both cortical and thalamic recordings.

Spindle detection

We applied an existing spindle detector with robustness to epileptic spikes and sharp transients.[31] Given the wide age range of the subjects analysed, we used a detector that has been validated in both children and adults.[39] Briefly, the spindle detector estimates a latent state (the probability of a spindle) using three features: the Fano factor (estimated for data FIR filtered between 3 and 25 Hz), normalized power in the spindle band (9–15 Hz) and normalized power in the theta band (4–8 Hz). Distributions of expected values for these parameters were determined using manually detected spindles in the scalp EEG of subjects with sleep-activated spikes. To avoid misidentifying spikes as spindles, we applied a cubic spline to the ±50 ms interval around each detected spike before applying the spindle detector (as recommended by Klinzing *et al.*[30]). Doing so further improves the ability of the spindle detector to reject spikes and accurately identify the beginning and end of spindles. The spindle detector estimates the probability of a spindle in 0.5 s intervals (0.4 s overlap). We detected a spindle when the probability crossed 0.95, chosen by optimizing the sensitivity and specificity of the detector.[31] We retained spindles with a minimum duration of 0.5 s, a maximum duration of 5 s and separated by ≥0.5 s; spindles within 0.5 s of one another were merged into a single spindle detection. We visually confirmed that the method accurately detected sleep spindles in both scalp EEG and thalamic recordings.

Slow oscillation detection

We applied the algorithm described by Mölle and Born[40] to detect slow oscillations. Briefly, slow oscillations were detected by: (i) filtering the data (both backwards and forwards) into the 0.4–4 Hz band using an FIR filter (4092 order); (ii) identifying all negative to positive zero-crossings and the time interval (*t*) to the subsequent positive to negative zero-crossings; (iii) retaining all intervals of duration $0.5\,s \leq t \leq 2\,s$ (corresponding to oscillations 0.5–2 Hz) and identifying the negative peak and peak-to-peak amplitude; (iv) omitting intervals in the bottom 75th percentile of peak-to-peak amplitude and the bottom 25th percentile of the negative peak amplitude; and (v) retaining any remaining intervals as slow oscillations.

Statistical analysis

Point process models for slow oscillations, spikes and spindles

To test hypotheses about relationships between slow oscillations, epileptic spikes and thalamic or scalp spindles, we first represented the event detections as a sequence of discrete events or point process time series. These stochastic point process time series are completely characterized by the conditional intensity function, representing the history-dependent generalization of the rate function of a Poisson process,

$$\lambda(t\,|H_t) = \lim_{\Delta\to 0}\frac{P[N_{t+\Delta} - N_t = 1\,|H_t]}{\Delta} \quad (1)$$

where P is a conditional probability, N_t denotes the number of events counted in the time interval (0, t] and H_t includes the event history up to time t and other covariates.[41] The logarithm of the conditional intensity, when considering a time-discretized point process, can be expressed as a linear function of covariates,

$$\log\lambda(k|H_k) = \beta_0 + \sum_{i=1}^{Q}\gamma_i\,\Delta N_{k-i} + \sum_{i=-n}^{n}\beta_i\,\Delta N^c_{k-i} \quad (2)$$

where k is the k^{th} interval of discretized time (with $k > Q$ and $k > n$), the first term (β_0) represents a baseline event rate, the second term represents a self-history autoregressive process and the third term represents past and future contributions from other covariates. The expressions $\Delta N_k = N_{t_{k+1}} - N_{t_k}$ and $\Delta N^c_k = N^c_{t_{k+1}} - N^c_{t_k}$ indicate binary time series of increments in event counts, and (β_i, γ_i) are parameters to estimate. This discrete-time point process likelihood function is equivalent to the likelihood of a generalized linear model under a Poisson distribution and log-link function.[41] We estimated model parameters using the *fitglm* function in MATLAB.

Modelling slow oscillations, cortical spikes and thalamic or scalp spindles

To characterize the relationship between scalp slow oscillations and cortical epileptic spikes, we divided time into 0.125 s intervals and created two binary time series. In the first time series, a value of 1 was assigned to intervals containing the down-state of a slow oscillation and 0 otherwise. In the second time series, a value of 1 was assigned to intervals containing the maximum amplitude of an epileptic spike, and 0 otherwise. When more than one epileptic spike occurred in the same 0.125 s interval, the value of that interval was set to the number of spikes that occurred. Using these point process time series, we estimated the model:

$$\log\ \lambda_{SSO}(k|H_k) = \beta_0 + \sum_{i=1}^{Q} \gamma_i\ \Delta N_{k-i}^{SSO} + \sum_{i=-n}^{n} \beta_i\ \Delta N_{k-i}^{CES} \quad (3)$$

where $\lambda_{SSO}(k|H_k)$ represents the conditional intensity or conditional event rate of scalp slow oscillations (SSO) given the history of SSO events and the occurrence of cortical epileptic spikes (CES) at past and future times.

In the same way, to characterize the relationship between scalp slow oscillations and thalamic spindle oscillations, we created point process times series and estimated the conditional event rate of scalp slow oscillations. For spindle detections, we assigned each 0.125 s interval a value of one if the maximum amplitude of a spindle occurred, or zero otherwise. Slow oscillations and spindle oscillations were modelled using:

$$\log\ \lambda_{SSO}(k|H_k) = \beta_0 + \sum_{i=1}^{Q} \gamma_i\ \Delta N_{k-i}^{SSO} + \sum_{i=-n}^{n} \beta_i\ \Delta N_{k-i}^{TSp} \quad (4)$$

where $\lambda_{SSO}(k|H_k)$ represents the conditional intensity or conditional event rate of scalp slow oscillations (SSO) given the history of SSO events and the occurrence of thalamic spindles (TSp) at past and future times. We applied the same model to assess the relationship between slow oscillations and scalp spindles by replacing ΔN_{k-i}^{TSp} with ΔN_{k-i}^{SSp}, the history and future of scalp spindle occurrences.

Using these models, we estimated the phase relationships between slow oscillations, spikes and spindles. We note that the prediction of the scalp slow oscillation down-state using cortical spikes and thalamic spindles is not causal. We chose this model structure to assess the temporal relationship of spikes and spindles to the slow oscillation down-state in a manner concordant with past work.[42]

For all models, we tested the model improvement relative to a nested model with only the history of the scalp slow oscillations. To estimate parameter significance within a model, we applied the Wald test. Confidence intervals for the parameters were estimated from the model fits using the function *fitglm* in MATLAB. Finally, we tested hypotheses across groups of parameters[43] using an *F*-test implemented in the *coefTest* function in MATLAB.

Procedures to estimate cortical spike propagation to thalamus

To test the hypothesis that cortical epileptic spikes propagate to the thalamus, we estimated: (i) the average thalamic evoked response; (ii) an unnormalized cross-correlation histogram; and (iii) the conditional event rate of thalamic spikes given cortical spikes. We define each measure here.

The average evoked response assumes a temporally locked relationship between cortical epileptic spikes and thalamic epileptic spikes. To assess this relationship, for each subject, we extracted from the thalamic voltage signal ±1 s intervals centred on the times of each cortical spike. We then estimated the mean thalamic response and standard error across all subjects and cortical spikes and tested the results against overlap with zero. Confidence limits were Bonferroni corrected for multiple comparisons.

To estimate the unnormalized cross-correlation histogram,[44] we first created binary time series using one to demarcate time points with the maximum amplitude of an epileptic spike and zero otherwise. Then we: (i) identified the time t_i of each event i from the cortical binary time series; (ii) identified the delays of all events in the thalamic binary time series in the interval ±1s around each t_i; and (iii) constructed a histogram from the temporal delays of thalamic spikes relative to the cortical spikes using ~35 ms bins. To assess the significance of the cross-correlation histograms, we created a null distribution of values by shuffling the inter-event intervals (i.e. time between events) of the cortical binary time series and then re-estimating the cross-correlation histograms. This process accounts for baseline rates of cortical spike occurrence and the distribution of inter-event intervals. We repeated this procedure 5000 times for each subject. Using the shuffled cross-correlation histograms, we created 95% confidence intervals (CI) for the null distribution and corrected for multiple comparisons (owing to the 60 bins, each of ~35 ms width) using Bonferroni correction. From the cross-correlation histogram, we computed the number of thalamic spikes in each time bin between [0,1] s after a cortical spike for each patient. To compare the mean number of thalamic spikes in the [0,1] s interval between groups (EE-SWAS, SWAS and non-SWAS), we modelled the mean number of thalamic spikes with an indicator for group (generalized linear model with log-link and a Gamma-distributed response). We compared the mean number of spikes between the EE-SWAS and non-SWAS groups and between SWAS and non-SWAS groups using the *coefTest* function in MATLAB.

Finally, to characterize the relationship between cortical epileptic spikes (CES) and thalamic epileptic spikes (TES), we divided the time series into 16 ms intervals (the lowest temporal resolution for epileptic spikes) and estimated the model,

$$\begin{aligned}\log \lambda_{TES}(t|H_t) = {} & \beta_0 + I_{EE-SWAS}\left(\sum_{i=1}^{k} \gamma_i^{EE-SWAS}\ \Delta N_{t-i}^{TES} + \sum_{i=-n}^{n} \beta_i^{EE-SWAS}\ \Delta N_{t-i}^{CES}\right) \\ & + I_{SWAS}\left(\sum_{i=1}^{k} \gamma_i^{SWAS}\ \Delta N_{t-i}^{TES} + \sum_{i=-n}^{n} \beta_i^{SWAS}\ \Delta N_{t-i}^{CES}\right) \\ & + I_{non-SWAS}\left(\sum_{i=1}^{k} \gamma_i^{non-SWAS}\ \Delta N_{t-i}^{TES} + \sum_{i=-n}^{n} \beta_i^{non-SWAS}\ \Delta N_{t-i}^{CES}\right)\end{aligned} \quad (5)$$

where the variable I indicates subject group (EE-SWAS, SWAS and non-SWAS), and we include the self-history of TES and the history and future of CES.

Procedures to estimate relationships between thalamic and scalp spindles

To test the hypothesis that thalamic spindles predict scalp spindles, we estimated: (i) the average evoked response at the scalp; (ii) the average induced response at the thalamus; and (iii) the conditional event rate of scalp spindles. We define each measure here.

To assess the average evoked response at the scalp, for each subject, we extracted from the scalp EEG signal ±2 s intervals centred on the times of the maximum amplitude of each thalamic

spindle. We then estimated the mean EEG response and standard error across all subjects and thalamic spindles and tested the results against overlap with zero. The confidence limits were Bonferroni corrected for multiple comparisons.

To estimate the average induced response at the thalamus, we applied a multitaper spectral analysis to estimate the spectrogram. For each subject, we first extracted from the thalamic signal ±2 s intervals centred on the times of the maximum amplitude of each scalp spindle. We then estimated the spectrogram of each extracted thalamic signal using 0.5 s intervals (0.45 s overlap) and a single taper (2 Hz frequency resolution, function mtspecgramc from the Chronux toolbox[45]). To enable testing and comparisons, we log-transformed and standardized (removed mean and divided by standard deviation) over time for each frequency of each spectrogram. We then averaged the spectrograms across all extracted signals (i.e. across all instances of scalp spindles for all subjects within each group) and tested the resulting power relative to zero using the estimated standard error.

To characterize the relationship between scalp spindles (SSp) and thalamic spindles (TSp), we estimated the model,

$$\log \lambda_{SSp}(t|H_t) = \beta_0 + \sum_{i=1}^{k} \gamma_i \Delta N_{t-i}^{SSp} + \sum_{i=-n}^{n} \beta_i \Delta N_{t-i}^{TSp} \quad (6)$$

where we include the self-history of scalp spindles to account for a spindle refractory period and identify the independent contribution of thalamic spindles. We identify binary spindle occurrences using time intervals of 0.125 s, where one indicates the maximum amplitude of a spindle that occurred (and zero otherwise).

Procedures to estimate relationships between epileptic spikes and spindles

To test the hypothesis that epileptic spikes disrupt spindles, we examined the relationship across two time scales. At the ultradian time scale, we compared the spindle and epileptic spike rates recorded at the scalp, cortex and thalamus. To do so, we computed for each subject the spindle and epileptic spike rates as the total number of events divided by the total duration of data analysed (i.e. total duration of N2). We then fitted a linear mixed-effects model of the spindle rates versus the log-transformed spike rates with patient as random effect. We tested the model against a nested model with constant predictor and random effect of patient using a likelihood ratio test implemented by the MATLAB function *compare*.

At the minutes time scale, we modelled the relationship between thalamic epileptic spikes (TES) and thalamic spindles (TSp) as

$$\log \lambda_{TSp}(t|H_t) = \beta_0 + \sum_{i=1}^{k} \gamma_i \Delta N_{t-i}^{TSp} + \sum_{i=-n}^{n} \beta_i \Delta N_{t-i}^{TES} \quad (7)$$

where we include the self-history of thalamic spindles to account for a possible refractory period and identify the independent contribution of thalamic epileptic spikes. Here, we identify binary time series for spindle events using time intervals of 1 s, where one indicates that the maximum amplitude of a spindle occurred in an interval. Likewise, we identify spike event time series by indicating the number of spikes (i.e. times of maximum amplitude of an epileptic spike) occurring in each 1 s time interval. We estimated the model considering self-history terms up to 20 s and thalamic epileptic spike terms up to ±60 s around each scalp spindle. Based on visual analysis, we expected that there could be an effect up to 30 s after a spike. To smooth the estimated parameters, the coefficients were tested in a group hypothesis test for the parameters between −35 and −25 s, −25 and −15 s, and −15 and −5 s, with 0 s indicating the event centre of a scalp spindle. We thus test whether $\sum \beta_{[-35,-25)} < 0$, $\sum \beta_{[-25,-15)} < 0$ or $\sum \beta_{[-15,-5)} < 0$ and correct for performing three tests with Bonferroni correction. We avoid testing the (−5, 5) s period around time 0 s owing to limitations with our spindle detection approach: because we identify the spindle occurrence by maximum amplitude of the spindle, a spindle can begin before 0 s.

To investigate the impact of thalamic spikes on scalp spindles, we estimated a similar model between thalamic epileptic spikes (TES) and scalp spindles (SSp),

$$\log \lambda_{SSp}(t|H_t) = \beta_0 + \sum_{i=1}^{k} \gamma_i \Delta N_{t-i}^{SSp} + \sum_{i=-n}^{n} \beta_i \Delta N_{t-i}^{TES} \quad (8)$$

where we include the self-history of scalp spindles to account for a possible refractory period and identify the independent contribution of thalamic epileptic spikes. We performed the same statistical tests for this model as for the model of thalamic spindles.

At the seconds time scale, we compared the refractory periods of thalamic and scalp spindles with intervening thalamic epileptic spikes and without. Refractory periods were defined as the duration between the end of one spindle and the beginning of another. We fitted the distributions of the refractory periods using a generalized linear model with a log-link and an inverse Gaussian distributed response and compared the means of the two refractory period distributions using the function *coefTest* in MATLAB.

Results

Subject and data characteristics

Nine subjects (ages 9–55 years, two female; see clinical and data characteristics in Table 1) undergoing simultaneous scalp EEG and stereoelectroencephalography (SEEG) sampling of cortex and thalamus were included. For each subject, bipolar thalamic depth electrode contacts, bipolar cortical depth electrode contacts in the clinically determined seizure onset zone and bipolar scalp electrode contacts (CZ–PZ) were analysed. For slow oscillation detection and analysis, the scalp electrode CZ was analysed referenced to a far-field reference (the second spinous process, routinely used clinically at our institution). We classified subjects into three groups following the International League Against Epilepsy (ILAE) electroclinical criteria for diagnosis of EE-SWAS. Three subjects had both marked increase in spike activity during sleep and clinically identified cognitive plateau, regression or deceleration[5] (EE-SWAS); three subjects had a marked increase in spike activity during sleep without cognitive symptoms (SWAS); and three subjects had neither markedly increased spike activation during sleep nor cognitive symptoms (non-SWAS). The spike rates during N2 sleep for each group at the scalp, cortex and thalamus are provided in Supplementary Table 1.

Cortical slow oscillations predict both epileptic spikes and sleep spindles at different phases

In contrast to wakefulness, non-REM sleep is dominated by slow oscillations. To understand the influence of slow oscillations on sleep spindles (a canonical rhythm of N2 sleep) and epileptic spikes (activated during sleep in SWAS), we analysed the temporal and phase

relationships of slow oscillations to epileptic spikes and sleep spindles during N2 sleep (examples in Fig. 1A). Applying a statistical modelling approach (Fig. 1B), we find that scalp slow oscillations ($n = 42\,041$ events) increase the probability of a co-occurring cortical epileptic spike [$n = 65\,107$ events, nested model test $\chi^2(64) = 5646.5$, $P \approx 0$] and also, in an independent model, thalamic sleep spindles [$n = 14\,845$ events, nested model test $\chi^2(64) = 195.04$, $P = 3.6 \times 10^{-15}$; see the 'Materials and methods' section]. Averaging all detected slow oscillations across all nine subjects, the first up-state of the slow oscillation begins 1.4 s (range 0.88–1.61 s; defined as deviating from a baseline of 0 μV, Bonferroni corrected) before the down-state trough (i.e. at time −1.4 s in Fig. 1B). Here, we refer to the downward deflection between two zero-crossings in the slow oscillation as the down-state because this deflection has been related to decreased neuronal activity in prior work.[46,47] Cortical epileptic spikes increase (see the 'Materials and methods' section) from −1.125 to −0.125 s before the trough of the down-state (peak rate at −0.25 s before the down-state trough; Fig. 1B, top and bottom), during the up-state to down-state transition of the slow oscillation. In contrast, thalamic sleep spindles increase 0.25–0.875 s after the trough of the down-state (maximally detected 0.5 s after the down-state), during the up-state of the slow oscillation. Thus, when slow oscillations co-occur with spikes or when slow oscillations co-occur with spindles, slow oscillations are evident first. Analysing the same data using a non-parametric approach, we find consistent results (Fig. 1C); cortical spikes precede the down-state trough of the slow oscillation and thalamic spindles follow the down-state trough of the slow oscillation. From these results, cortical slow oscillations appear to predict both epileptic spikes and sleep spindles, where epileptic spikes maximally occur earlier in the slow oscillation than sleep spindles. To investigate whether spikes are impacting slow oscillations, we now analyse slow oscillation morphology in the presence or absence of local spikes versus distant spikes.

We note that in our analysis slow oscillations were measured at the scalp vertex (CZ), while focal cortical spikes were measured at epileptic foci variably located across subjects in the intracranial SEEG recording (Table 1). To evaluate whether co-occurring epileptic spikes might be impacting the morphology of the slow oscillation, we further investigated the relationship between cortical slow oscillations and epileptic spikes in two ways. First, we compared the average standardized scalp slow oscillations with or without co-occurring focal spikes in the same location (scalp EEG) and with and without co-occurring focal spikes in a distant location (intracranial). We found that slow oscillations with and without co-occurring spikes had nearly the same morphology (waveform $R^2_{Scalp} = 0.95$, $R^2_{Cortex} = 0.98$), although the slow oscillations with co-occurring spikes at any location (scalp or intracranial) had a slightly deeper down-state than slow oscillations without co-occurring spikes (scalp: −0.45 standard units difference; cortex: −0.62 standard units difference; Fig. 2A). In contrast, we found that slow oscillation morphology was the same (confidence intervals overlap throughout waveform) when comparing slow oscillations with co-occurring local spikes (scalp EEG) versus distal spikes (intracranial EEG) ($R^2_{Scalp:Cortex} = 0.97$; Fig. 2B). These results suggest that epileptic spikes are more likely to co-occur with slow oscillations with a deeper down-state, but the presence of a focal spike does not measurably impact the slow oscillation morphology.

Second, we investigated the relationship between spindles and slow oscillations with or without co-occurring cortical spikes. We found that slow oscillations with and without cortical spikes both positively modulated thalamic spindle rates (from 0.125 s to 0.75 s in Fig. 2C). With cortical spikes, there was, on average, an upregulation of 1.16 (95% CI: 1.1–1.22, $P = 5.4 \times 10^{-9}$); without cortical spikes, there was an upregulation of 1.15 (95% CI: 1.07–1.22, $P = 3 \times 10^{-5}$). We conclude that scalp slow oscillations with cortical spikes continue to modulate thalamic spindle rates. However, for slow oscillations co-occurring with thalamic spikes, we find decreased thalamic spindle rates on average between 0.125 and 0.75 s (orange curve in Fig. 2D; factor of 0.83, 95% CI: 0.74–0.94, $P = 0.0031$). We note that slow oscillations without thalamic spikes positively modulated thalamic spindle rates, as expected (green curve in Fig. 2D; factor of 1.23, 95% CI: 1.18–1.28, $P = 3.2 \times 10^{-21}$). We conclude that thalamic spikes impact thalamic spindle occurrence more than focal cortical spikes do.

These results show that cortical slow oscillations predict both epileptic spikes and sleep spindles, where epileptic spikes occur maximally earlier in the slow oscillation than sleep spindles and epileptic spikes in the thalamus disrupt thalamic spindles. We note that, when the combined modulatory roles of slow oscillations, cortical spikes or thalamic spikes on spindles are ignored, focal cortical spikes appear to induce spindles (Figs 1B and 2C and Supplementary Fig. 1). These results help to explain why epileptic spikes and spindles are both prominent in non-REM sleep: both spikes and spindles co-occur with the slow oscillations prominent in N2 sleep. In addition, these results support the hypothesis that pathological epileptic spikes in the thalamus 'hijack' the same slow oscillatory circuitry that supports physiological sleep spindles.

Cortical spikes precede and predict thalamic spikes

Animal models suggest that epileptiform spikes initiate in the cortex,[25] and clinical observations suggest that epileptiform activity can propagate to the thalamus.[48] To assess these observations here, we applied cross-correlation histograms to all detected cortical epileptic spikes ($n = 65\,107$ events) and thalamic epileptic spikes ($n = 15\,250$ events) during N2 sleep. We found that, across subjects and groups, thalamic spikes tend to occur immediately after cortical spikes (Fig. 3A and B). This relationship is most prominent in subjects with EE-SWAS and SWAS, in whom a higher mean number of thalamic spikes occurred within 1 s of a cortical spike, compared to subjects without SWAS (F-test, $P = 4 \times 10^{-20}$ and $P = 6 \times 10^{-20}$, respectively; see the 'Materials and methods' section). To assess the relationship between cortical and thalamic spike occurrence across all subjects, we developed a generalized linear model for the time series of detected events (see the 'Materials and methods' section). We found that, after accounting for spike history, the thalamic spike rate increases 8–40 ms after a cortical spike [nested model test $\chi^2(27) = 5548.1$, $P \approx 0$; Fig. 3C]. Indeed, in each group, cortical spikes increase the likelihood of thalamic spikes (Fig. 3C), although these events are sparse in the non-SWAS group. We note that, in Fig. 3C, the horizontal axis indicates the time of a cortical spike relative to a thalamic spike at time 0 s; negative times indicate cortical spikes that precede thalamic spikes. To evaluate further for evidence of cortical to thalamic spike propagation, separate from possible contributions attributable to slow oscillation propagation, we generated the cross-correlation histogram after removing all spikes in the thalamus and cortex that occurred within 500 ms of a slow oscillation down-state. We found a consistent result: thalamic spikes most frequently occurred within 30 ms after a cortical spike (Supplementary Fig. 2). Thus, a cortical spike during N2 sleep predicts a rapid subsequent thalamic spike, consistent with corticothalamic propagation.

Thalamic spikes inhibit sleep spindles

Although existing models suggest that epileptic spikes disrupt spindles,[4,49,50] no direct observations of this disruption exist in

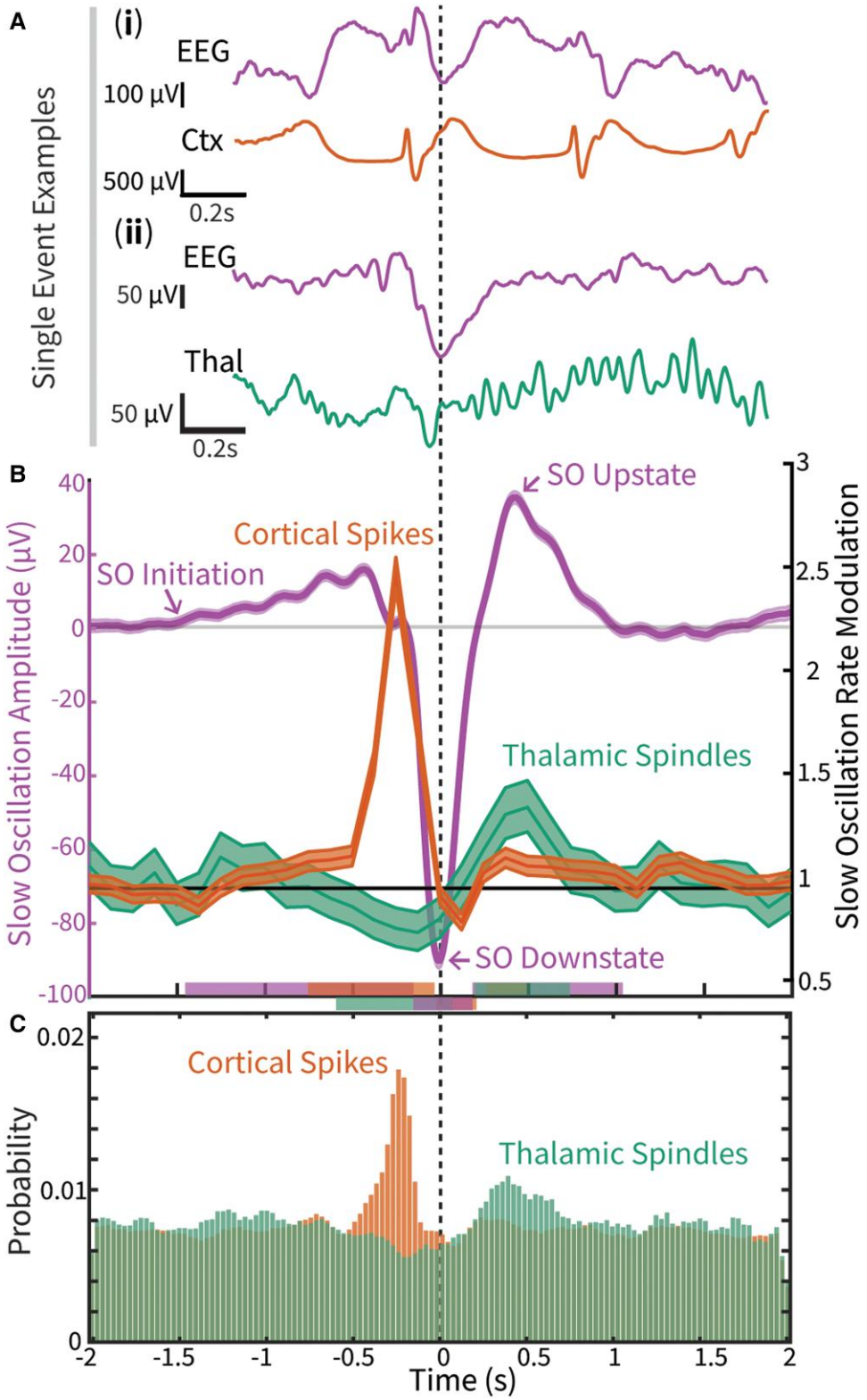

Figure 1 Slow waves predict spikes and spindles at different phases. (**A**) Example simultaneous recordings of scalp EEG (purple traces), cortical stereo-electroencephalography (SEEG; orange trace) and thalamic SEEG (green trace) centred on slow oscillation down-state troughs (vertical dashed line). [**A(i)**] A cortical spike (orange trace) precedes the down-state. [**A(ii)**] A thalamic sleep spindle (green trace) follows the down-state. (**B**) Averaged cortical slow oscillations (SO) low-pass filtered below 30 Hz (purple) across all subjects. Slow waves initiate with a low-amplitude up-state ~1.4 s before the down-state trough. The modulation coefficient (95% confidence interval) of cortical spike rate (orange) and thalamic spindle rate (green) is shown over the course of the slow oscillation. Spikes are positively modulated during the up-state to down-state transition. Sleep spindles are positively modulated during the up-state. Horizontal bars on the bottom axis indicate times during which the slow oscillation amplitude (purple), spindle rate modulation (green) and spike rate modulation (orange) are significant ($P < 0.05$). (**C**) Normalized cross-correlation histogram of events timed to down-state at 0 s reflecting the modulation of cortical spikes and thalamic spindle occurrences.

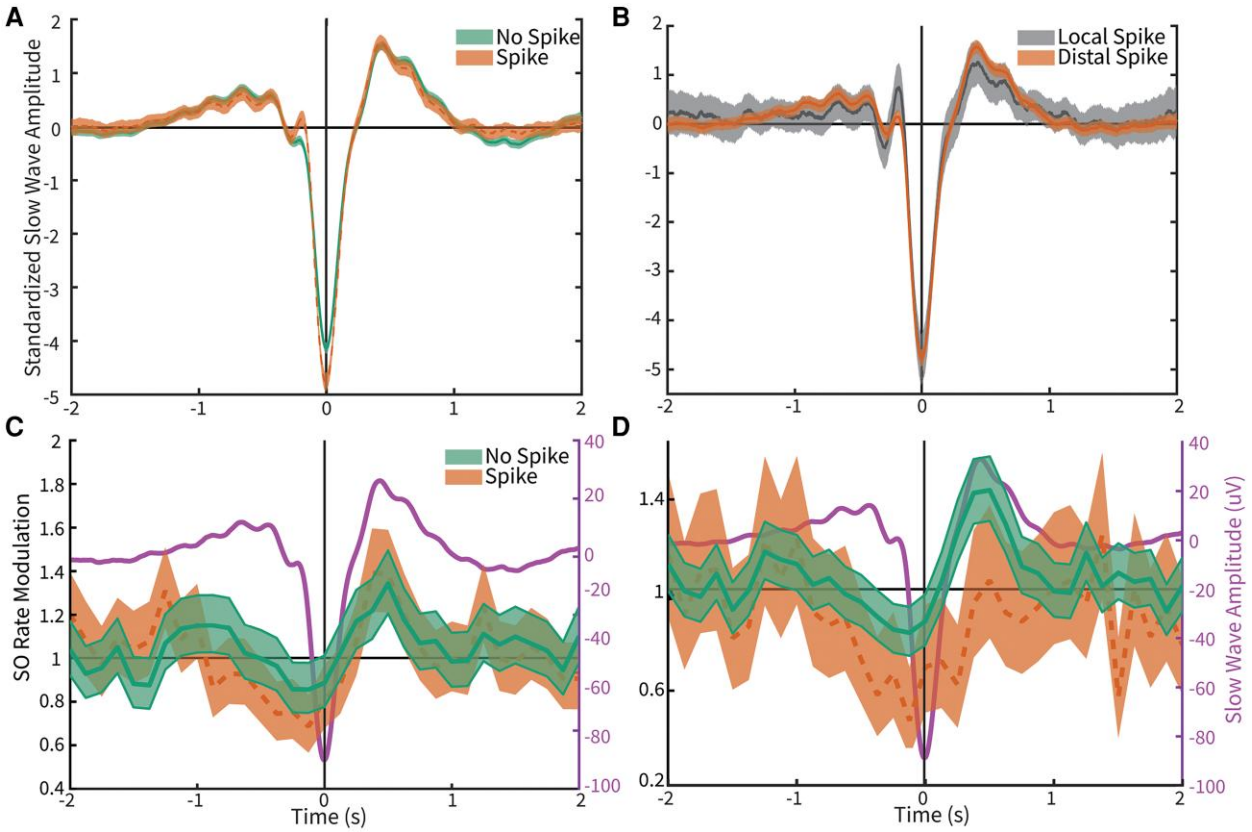

Figure 2 Slow oscillations with or without cortical spikes exhibit similar dynamics and impact on thalamic spindles. (**A**) Averaged unfiltered slow oscillations (SO) that did [orange; shaded area indicates 95% confidence intervals (CI)] or did not (green; shaded area indicates 95% CI) co-occur with a distant cortical spike. (**B**) Averaged unfiltered slow oscillations that co-occurred with a local scalp EEG spike (grey; shaded area indicates 95% CI) or with a distant cortical intracranial spike (orange; shaded area indicates 95% CI). (**C**) Thalamic spindle modulation (95% CI) for slow oscillations with (orange) and without (green) cortical spikes. Averaged slow oscillations are shown in purple. Spindles occur maximally during the slow oscillation up-state. (**D**) Same as **C**, but for thalamic spikes instead of cortical spikes. Thalamic spindles are significantly decreased on average for slow oscillations with thalamic spikes during the slow oscillation up-state between 0.125 and 0.75 s (see main text for details).

humans. To address this, we evaluated the relationship between epileptic spikes and sleep spindles across scalp, cortical and thalamic recordings. Consistent with previous observations,[31,33,51] evaluating across three separate regions per patient (scalp, intracranial cortex near the seizure onset zone and thalamus; see the 'Materials and methods' section), we found that the epileptic spike rate and sleep spindle rate across N2 sleep were anti-correlated ($r = -0.59$; $P = 0.0015$; Fig. 4A and B). In support of this observation, in each group, thalamic spindle refractory periods were longer if a thalamic spike occurred between spindles (EE-SWAS: 4.27 ± 0.1 s; SWAS: 2.66 ± 0.02 s; non-SWAS: 3.48 ± 0.1 s) compared with thalamic spindle refractory periods with no intervening thalamic spike (EE-SWAS: 2.39 ± 0.02 s; SWAS: 1.81 ± 0.02 s; non-SWAS: 2.38 ± 0.02 s; $P \approx 0$, $P \approx 0$ and $P = 1.1 \times 10^{-27}$, respectively; Fig. 4C; see the 'Materials and methods' section).

To characterize further the inhibitory effect of thalamic spikes on spindles, we modelled the thalamic spindle event rate using the history of thalamic spindles and thalamic spikes as predictors (see the 'Materials and methods' section). In the EE-SWAS group, the likelihood of a thalamic sleep spindle was significantly decreased in the period immediately after a thalamic spike (Fig. 4C and D). The presence of a thalamic spike from –35 to –15 s before a spindle decreased the probability of a thalamic spindle by a factor of 0.91 (for –35 to –25 s, factor of 0.92, 95% CI: 0.86–0.98, $P = 0.0098$; for –25 to –15 s, factor of 0.9, 95% CI: 0.84–0.97, $P = 0.0014$; for –15 to –5 s, factor of 0.94, 95% CI: 0.88–0.99, $P = 0.033$); we found qualitatively similar results for spikes that did or did not co-occur with slow oscillations (Supplementary Fig. 3). The downregulation of thalamic spindles was maximal ~10 s after a thalamic spike (by a factor of 0.71, 95% CI: 0.56–0.94, $P = 0.013$). This prolonged effect was detected only in the EE-SWAS group. For this analysis, we omit times immediately before a spindle (–5 to 0 s) owing to the temporal limitations of our spindle analysis approach (e.g. spindle rate at time zero here is the time of the maximum amplitude of the sigma amplitude of detected spindles, which can be mid-spindle). Thus, we find that thalamic spikes increase the spindle refractory period in all patient groups and downregulate the probability of a thalamic spindle for tens of seconds in patients with epileptic encephalopathy and spike activation during sleep.

We find consistent results for the relationship between thalamic spikes and scalp-detected sleep spindles (Fig. 4E and F). In all groups, we find increased scalp spindle refractory periods when a thalamic spike occurred between spindles (EE-SWAS: 4.82 ± 0.34 s; SWAS: 3.23 ± 0.08 s; non-SWAS: 2.84 ± 0.22) compared with spindle refractory periods without an intervening thalamic spike (EE-SWAS: 2.71 ± 0.08 s; SWAS: 1.84 ± 0.04 s; non-SWAS: 1.74 ± 0.02 s, $P \approx 0$, $P \approx 0$ and $P = 1.5 \times 10^{-21}$, respectively; Fig. 4E). For subjects with EE-SWAS, modelling scalp spindle events with the predictors thalamic spike events and self-history (i.e. scalp spindle events; see the 'Materials and methods' section), we find downregulation of scalp spindles following thalamic spikes (for –25 s to –15 s, factor of 0.86, 95% CI: 0.77–

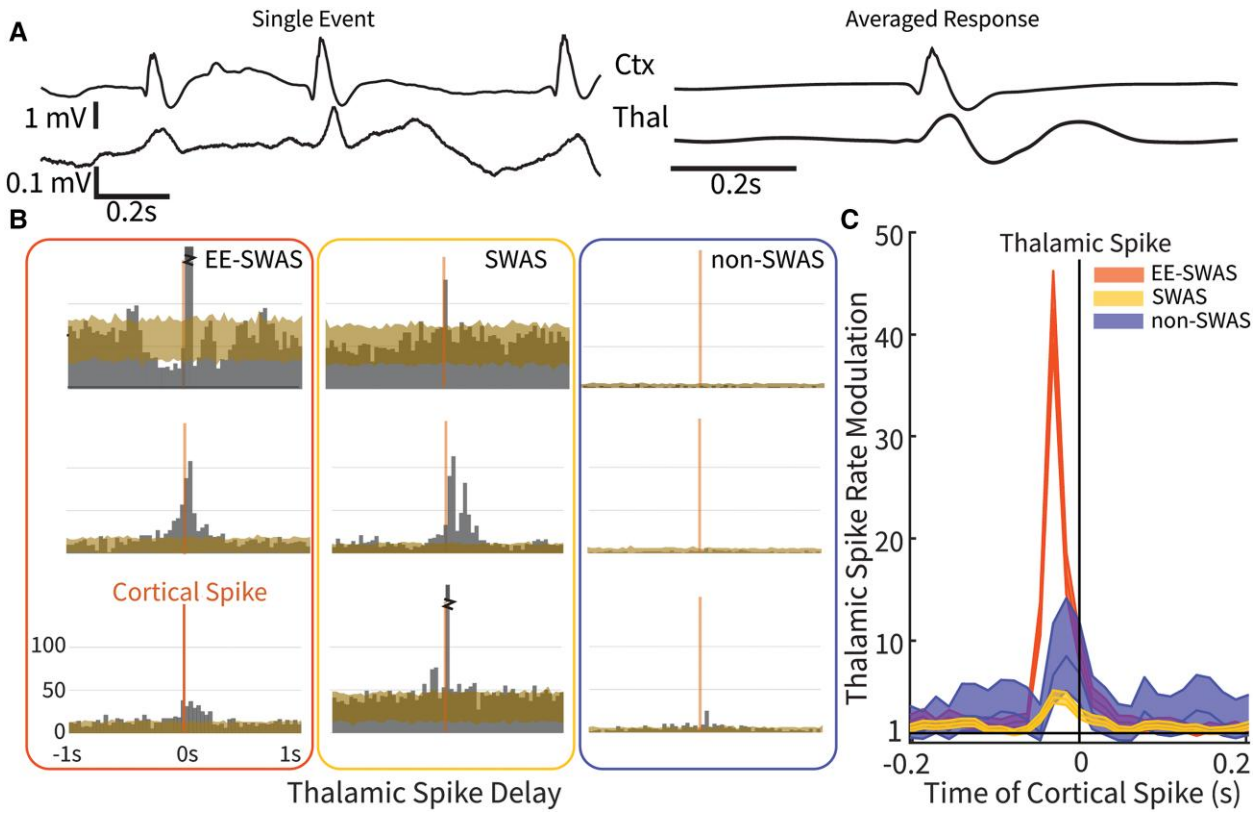

Figure 3 Cortical spikes drive thalamic spikes in subjects with spike and wave activation in sleep (SWAS). (**A**) Example epileptic spikes (*left*) from one subject in the cortex (Ctx) and thalamus (Thal) and (*right*) the averaged response time locked to cortical spikes. (**B**) Cross-correlation histograms of thalamic spikes relative to the time of cortical spikes for each subject. Zero indicates the moment of a cortical spike. (**C**) Model estimates of thalamic spike rate modulation attributable to the occurrence of a cortical spike (mean solid, confidence intervals shaded) for each patient group (see key). Significant increases [$P < 0.05$ when confidence intervals exclude one (black horizontal line)] in thalamic spike rate occur owing to a preceding (8–40 ms earlier) cortical spike.

0.94, $P = 0.0016$; for −15 to −5 s, factor of 0.75, 95% CI: 0.67–0.84, $P = 6.6 \times 10^{-7}$; Fig. 4F). Scalp spindles were maximally downregulated by a factor of 0.4 (95% CI: 0.23–0.69, $P = 0.0011$) when occurring ~5.5 s after a thalamic spike. This contrasts with results for thalamic spindles, where we observed a maximum downregulation at 10 s. One explanation for this difference is that the scalp EEG measures activity from a broader area of cortex, with the possibility of alternative thalamic spindle generators, than the thalamic nucleus sampled. This effect was detected only in the EE-SWAS group. We conclude that, across subjects, thalamic spikes increase sleep spindle refractory periods. Furthermore, in patients with EE-SWAS, thalamic spikes disrupt sleep spindles measured at the scalp.

Spindles co-occur in thalamus and scalp EEG

Sleep spindles are generated in thalamic circuitry and transmitted to the cortex, at least partly in response to cortical input.[4,50] To confirm that thalamocortical spindle propagation was consistent across subject groups using direct thalamic recordings in humans, we examined the averaged scalp activity time locked to the occurrence of thalamic spindles (see the 'Materials and methods' section). Thalamic spindles and scalp spindles co-occurred and were phase locked (Fig. 5A). We found higher spindle-band power in the thalamic data at the time of scalp spindles (Fig. 5B) for all patient groups (standardized spectrogram power $P < 0.05$). When modelling the scalp spindle event times using the thalamic spindle event times (and past scalp spindle occurrence, thus accounting for scalp spindle refractory periods), we found that thalamic spindles modulated scalp spindle rate [EE-SWAS: $\chi^2(20) = 138.28$, $P \approx 0$; SWAS: $\chi^2(20) = 844.52$, $P \approx 0$; non-SWAS: $\chi^2(20) = 1230.8$, $P \approx 0$] across all patient groups. A thalamic spindle increased the probability of a scalp spindle by a factor of 3.3 (95% CI: 2.4–4.7, $P = 3 \times 10^{-12}$) in EE-SWAS subjects, by a factor of 4.6 (95% CI: 3.9–5.5, $P \approx 0$) in SWAS subjects and by a factor of 3.1 (95% CI: 2.7–3.6, $P \approx 0$) in non-SWAS subjects. When temporally indexed to slow oscillations (Supplementary Fig. 4), the maximum modulation in the thalamic spindle rate (~0.5 s after slow oscillation down-state) preceded the maximum modulation in the scalp spindle rate (~0.625 s after slow oscillation down-state). We conclude that, across all groups, thalamic sleep spindle occurrence consistently modulates cortical sleep spindle occurrence, as expected. This finding is clinically significant, because non-invasive sleep spindle measures using scalp EEG accurately reflect spindle activity occurring in the thalamus.

Conceptual model of spike-driven epileptic encephalopathy

Taken together, our analyses support a unifying mechanistic circuit model of epileptic encephalopathy with spike-wave activation during sleep (Fig. 6). Slow oscillations, generated in the cortex, create conditions in the brain that facilitate corticothalamic spikes and

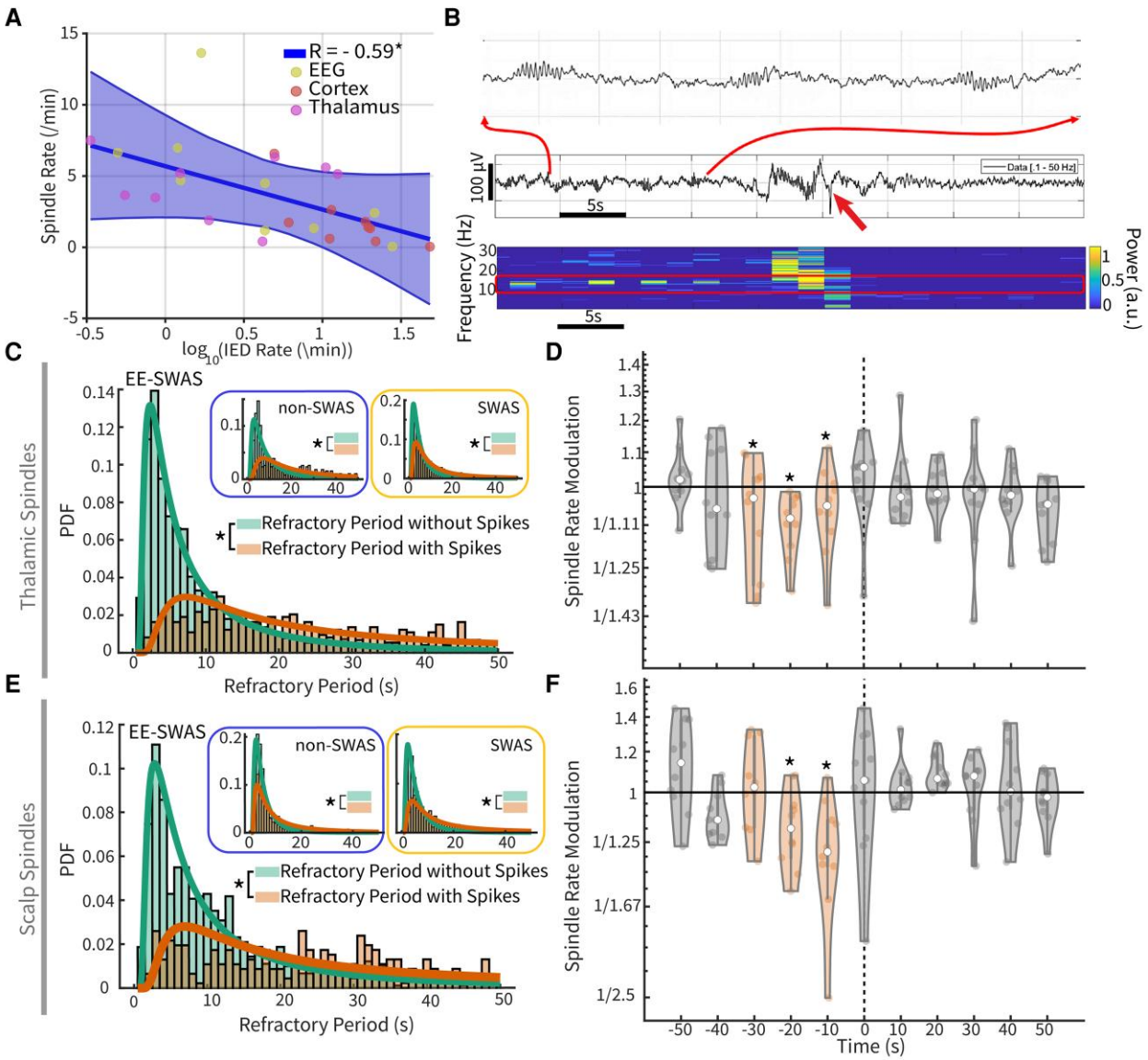

Figure 4 Spikes inhibit spindles. (**A**) Spike rate and spindle rate across subjects and brain regions during stage two (N2) sleep are anti-correlated. (**B**) Example spike disruption of spindles in the thalamus. Before a spike (red arrow), spindles occur regularly; see upper trace for example spindles and lower image for spindle band peaks in the spectrogram. After a spike, spindles are not apparent in the trace (*middle row*) or spectrogram (*bottom row*). (**C**) Histograms of thalamic spindle refractory periods with (orange) and without (green) intervening thalamic spikes for subjects with epileptic encephalopathy. *Insets* show distributions for subjects with (yellow) and without (blue) spike-wave activation during sleep (SWAS). (**D**) The rate of thalamic spindles is reduced by thalamic spikes in subjects with epileptic encephalopathy-related SWAS (EE-SWAS). Estimates of spindle rate modulation parameters at each second (coloured dots) and grouped over 10 s intervals (violin plots with median and quartiles indicated). Thalamic spindle rates are downregulated when a preceding spike occurs between −35 and −5 s. Time 0 s (dashed vertical line) indicates the time of spindle occurrence. (**E** and **F**) Same as in **C** and **D**, except using scalp EEG-detected spindles. In **F**, scalp spindle rates are downregulated when a preceding spike occurs between −25 and −5 s. $^{*}P < 0.05$.

thalamocortical spindles. The up-state to down-state transition of the slow oscillation promotes pathological epileptic cortical spikes. Sleep-facilitated epileptic spikes are more likely to propagate to the thalamus, resulting in increased thalamic spikes in patients with EE-SWAS. Simultaneously, the down-state to up-state transition of a slow oscillation facilitates thalamic sleep spindles, which peak at the subsequent up-state of the slow oscillation. These thalamic spindles propagate to the cortex and are observable in the scalp EEG. Epileptic spikes present in the thalamus induce a longer refractory period for spindles and can disrupt sleep spindle production more markedly in subjects with EE-SWAS.

In line with the observed statistical relationships that we report between sleep-activated cortical spikes, thalamic spikes and spindle suppression proposed by our model, we note anecdotally that one of the patients with EE-SWAS underwent cortical resection of the cortex with maximal spike activation during sleep. Following cortical resection, scalp cortical spindle rate increased nearly 5-fold during N2 on a night after resection compared with immediately before resection (0.24/min compared with 0.05/min, respectively). Thus, in this subject, resolution of the sleep-activated cortical spikes corresponded to increased sleep spindle production. Although further work is required to demonstrate causal relationships, this spike-disrupted

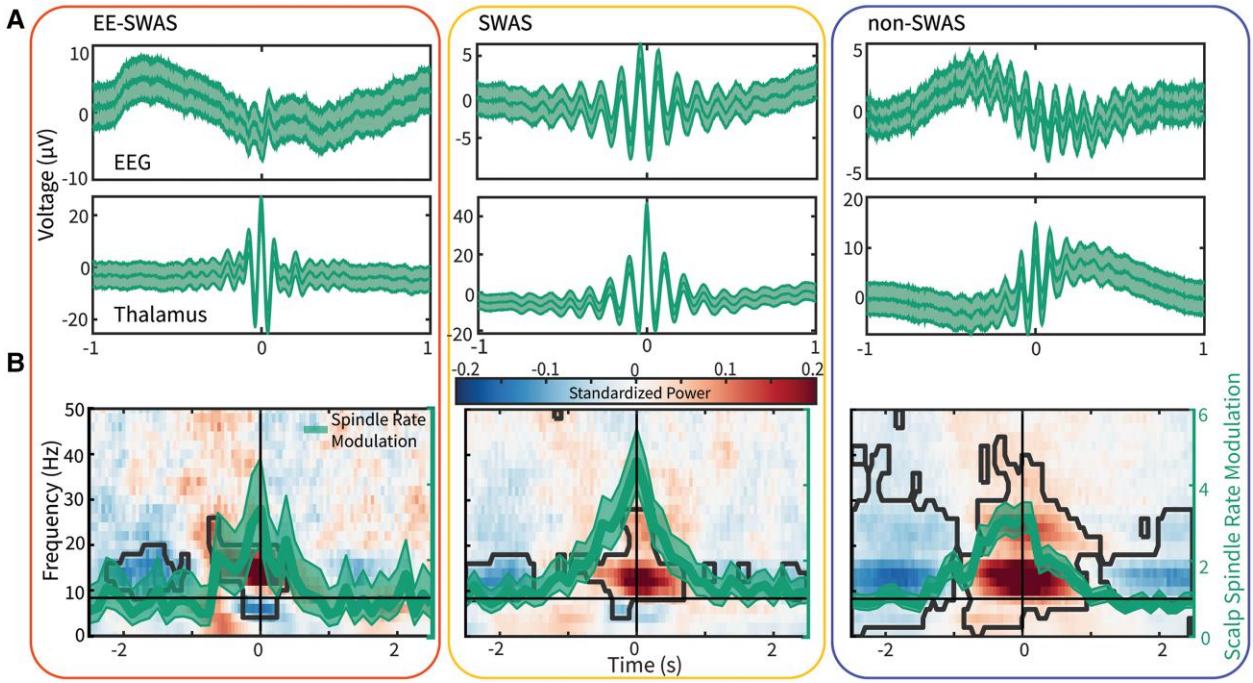

Figure 5 Spindles consistently co-occur in the thalamus and the scalp EEG across all subject groups. (**A**) Averaged spindle response in individual subjects, time locked to maximum spindle amplitude in the thalamus, indicates consistent phase-locked spindle activity across the cortex and thalamus. (**B**) Modulation of scalp spindle rate at time 0 s across subjects in each group (green curves, mean solid, 95% confidence intervals shaded) by thalamic spindles. Background spectrograms of thalamic data time locked to scalp spindles. Warm (cool) colours include high (low) standardized power; see scale bar. Regions outlined in black indicate Bonferroni-corrected islands of significant changes in power. EE = epileptic encephalopathy; SWAS = spike-wave activation during sleep.

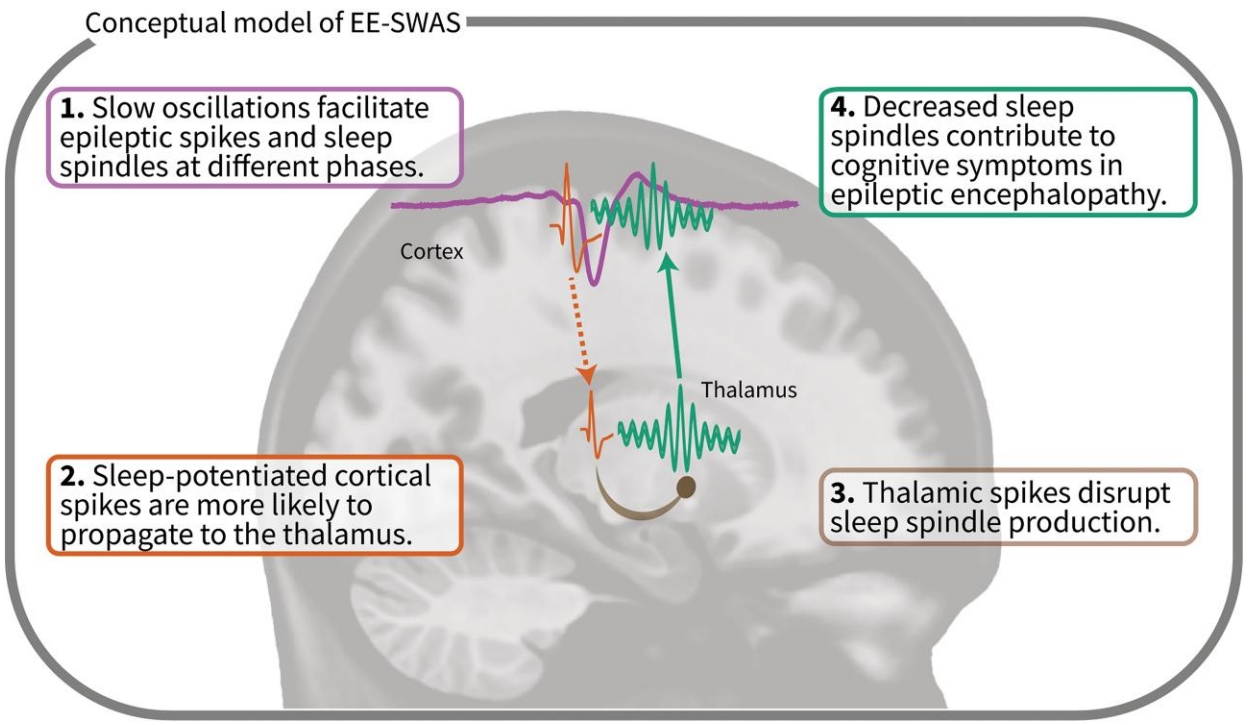

Figure 6 Proposed mechanistic circuit contributing to spindle deficit and cognitive dysfunction in epileptic encephalopathy associated with spike-wave activation during sleep (EE-SWAS). Our observations are consistent with this proposed mechanistic circuit.

electrophysiological circuit demonstrates a candidate mechanism for cognitive dysfunction in epilepsy.

Discussion

Cognitive symptoms are a common comorbidity in epilepsy, but there are currently no mechanisms to explain cognitive dysfunction or treatments to improve these dysfunctions. Although an underlying aetiology can often result in both epilepsy and cognitive dysfunction, and antiseizure medications themselves can contribute to cognitive dysfunction, epileptic encephalopathies are disorders in which the abnormal epileptic activity is thought to contribute directly to cognitive dysfunction beyond these influences. Here, using direct thalamic and cortical human brain recordings in subjects with epileptic activity, we provide evidence for a long-proposed mechanism by which epileptic activity contributes to cognitive dysfunction by disrupting thalamic sleep spindles.

Slow oscillations are a ubiquitous phenomenon in non-REM sleep and have been implicated in the initiation of sleep spindles[13] and the facilitation of epileptic spikes.[42] Inhibitory neurons may be coordinated by the slow oscillation up-state to help generate the down-state, and this increase in synchrony might, pathologically, facilitate an epileptic spike (for a discussion, see Frauscher *et al.*[29,42]). In our analysis, when slow oscillations co-occur with epileptic spikes, the first up-state of the triphasic slow oscillation (which has been linked to an increase in neuronal population activity[46]) precedes the epileptic spike. Slow oscillations that support epileptic spikes have a slightly deeper down-state, whether an epileptic spike occurs locally or at a distant location. We conclude from these results that epileptic spikes have little impact on the slow oscillation morphology. Indeed, our data show that high-amplitude slow oscillations detected at the scalp midline can facilitate epileptic spikes at local or distal irritative cortical locations (e.g. scalp CZ, intracranial frontal, parietal or temporal), in line with past observations.[42] Future recordings of single-neuron or multi-unit data would help to confirm that slow oscillations with and without epileptic spikes reflect similar population-level activities.

We note that previous work has observed that hippocampal epileptic spikes precede both slow oscillations and sleep spindles in the prefrontal cortex.[37] In contrast, we analysed slow oscillations at the scalp relative to cortical epileptic spikes across diverse epileptogenic zones, consistent with Frauscher *et al.*[29,42] Thus, dynamics in the prefrontal cortex might be unique, given its monosynaptic connectivity to the hippocampus,[52] whereas slow oscillations facilitate epileptic spikes in other cortical regions in patients with epilepsy. One additional interpretation of the results could be that a potential fourth, unobserved rhythm initiates both the slow oscillation and the epileptic spike (e.g. a 0.02 Hz rhythm has been proposed to coordinate spindle occurrence and arousal[53]). This hypothesis remains to be tested in future work.

Across time scales and recording locations, spikes and spindles were anti-correlated. This analysis replicates and extends past studies that also observed an anti-correlation between spikes and spindles in scalp EEG[30,31,33,51] and in the hippocampus.[29] Although subjects with spike activation during N2 sleep had higher overall epileptic spike rates, subjects with spike wave activation during sleep and epileptic encephalopathy had the most prolonged inhibition of sleep spindles following thalamic spikes. Based on these results and evidence from past studies, one aspect of EE-SWAS that differs from SWAS is the suppression of sleep spindles.[29-31,33,51] Here, we propose that three separate dynamic patterns support epileptic encephalopathies: (i) slow oscillation facilitation of epileptic spikes; (ii) corticothalamic spike propagation; and (iii) inhibition of thalamic sleep spindles. The uncovering of the thalamic neurophysiology here helps to reconcile why some subjects can have near-continuous spike and wave activity during sleep with a range of cognitive symptoms, spanning from no detectable cognitive impact to subtle deceleration to profound cognitive regression.[3] Future work in animal models is required to confirm our empirical observations in humans and identify the specific biophysical mechanisms that support these interacting electrophysiological events.

The role of sleep spindles in cognitive function, especially memory consolidation, in healthy individuals is well established.[12,54,55] Inhibition of spindles might reduce opportunities for high-fidelity memory consolidation[56] through reactivation of neuronal patterns during hippocampal ripples.[20,57] In support of this claim, spindle deficits have been linked to cognitive dysfunction in epilepsy[6,31,49] and in response to treatment.[32] Thus, in subjects with epileptic encephalopathy, cognitive deficits might be explained, in part, by the reduction of sleep spindles. Alternatively, changes in slow oscillation features over the course of sleep have been linked to cognitive deficits in epileptic encephalopathy.[58,59] Distinguishing the separate and joint impacts of slow oscillations, sleep spindles, and their coupling, on cognitive dysfunction in epileptic encephalopathy remains to be studied. Given that slow oscillations and sleep spindles are easily accessible in the scalp EEG, measurements of these rhythms provide a direct mechanistic biomarker of the cognitive impact of epileptic spikes. Such a biomarker could support detection of at-risk subjects, measurements of treatment response and screening of cognitive therapeutics.

Past work suggests that epileptic spikes are pathological excitatory pulses,[24] and sleep spindle probability is regulated by activation of the thalamic reticular nucleus and the hyperpolarization of the thalamocortical neurons.[12] Both the thalamic reticular nucleus neurons and thalamocortical neurons have a refractory period after a spindle because of after-hyperpolarization[11] or after-depolarization,[60] respectively. We hypothesize that the excess excitation induced from epileptic spikes might reduce the sleep spindle probability by inducing increased depolarization of thalamocortical cells, an expectation that is consistent with a thalamocortical computational model.[61] Alternatively, spikes might act as *de facto* spindles by occurring through the same circuits[4,62] and thus enable a phase reset of the spindle refractory period (e.g. by simultaneously inducing after-depolarization of thalamocortical cells and after-hyperpolarization of the thalamic reticular neurons).

Like most analyses of intracranial human thalamic data, our analyses were limited to a small group of subjects. In addition, we restricted our analysis of the complex electrophysiological interactions between brain structures and rhythms to N2 sleep. Because we analysed subjects with a wide range of ages and epilepsies, we cannot provide a comprehensive assessment of how these results vary with patient features. However, despite this diversity of patient features, we found consistent patterns across the large numbers of slow oscillations, spindles and epileptic spikes analysed. Future work is necessary to extend the analyses conducted here to a larger sample of subjects and to N3 sleep. Furthermore, whether patients with EE-SWAS also exhibit increased spike propagation from cortex to thalamus during wakefulness or different states of vigilance in comparison to patients without SWAS remains a topic for future work. Here, we did not directly link electrophysiological features to specific cognitive measures in individual subjects. Instead, we grouped subjects using clinical diagnoses related to the severity of cognitive deficits and showed how electrophysiological features differed between diagnostic groups. Our findings are consistent with prior work linking cortical sleep spindle deficits to cognitive symptoms in epilepsy.[29-31,33,51] Future

work using behavioural assays is required to assess the relationship between the circuit outlined here that results in spindle deficits and cognitive dysfunction in EE-SWAS.

Thalamic recordings are sparse and chosen based on clinical demands. As such, we combined recordings from anterior and centromedian nuclei. However, to ensure that the results were less affected by the different nuclei, we selected cortical leads that showed near-instantaneous seizure propagation to the thalamic nuclei with SEEG recordings. Nonetheless, we observed that there were thalamic spikes that occurred earlier than cortical spikes. These spikes might be generated in the thalamus or propagate from another unobserved (cortical) region. Recent work[14] has suggested that there might be differences in which area receives slow oscillations from the cortex (centromedian) and which area generates slow oscillations (anterior nucleus). In the study by Schreiner *et al.*,[14] only 30% of neocortical slow oscillations were connected to anterior thalamic slow oscillations, suggesting that most neocortical slow oscillations might still be generated cortically.

Conclusion

We analysed simultaneous invasive thalamic and cortical human recordings and non-invasive scalp EEG to understand the relationships between sleep slow oscillations, sleep spindles and epileptic spikes. These results support a mechanism of cognitive dysfunction in epileptic encephalopathy, wherein epileptic spikes travel from the cortex to the thalamus, inhibit sleep spindles and thereby disrupt a neurophysiological rhythm underlying memory consolidation.

Data availability

The data that support this study are available on request. The data are not publicly available because they contain information that could compromise the privacy of the research subjects.

Funding

A.W. and M.A.K. were partially supported by National Institute of Neurological Disorders and Stroke R01EB026938. A.W. and C.J.C. were partially supported by National Institute of Neurological Disorders and Stroke R01NS115868. M.A.K was partially supported by National Institute of Neurological Disorders and Stroke R01NS110669. A.W., M.A.K. and C.J.C. are grateful for funding from the Epilepsy Foundation New England Blue Skies Award to support this work.

Competing interests

The authors report no competing interests.

Supplementary material

Supplementary material is available at *Brain* online.

References

1. Taylor J, Kolamunnage-Dona R, Marson AG, et al. Patients with epilepsy: Cognitively compromised before the start of antiepileptic drug treatment? *Epilepsia*. 2010;51:48-56.
2. Taylor J, Baker GA. Newly diagnosed epilepsy: Cognitive outcome at 5years. *Epilepsy Behav*. 2010;18:397-403.
3. Wickens S, Bowden SC, D'Souza W. Cognitive functioning in children with self-limited epilepsy with centrotemporal spikes: A systematic review and meta-analysis. *Epilepsia*. 2017;58:1673-1685.
4. Beenhakker MP, Huguenard JR. Neurons that fire together also conspire together: Is normal sleep circuitry hijacked to generate epilepsy? *Neuron*. 2009;62:612-632.
5. Specchio N, Wirrell EC, Scheffer IE, et al. International League Against Epilepsy classification and definition of epilepsy syndromes with onset in childhood: Position paper by the ILAE task force on nosology and definitions. *Epilepsia*. 2022;63:1398-1442.
6. Holmes GL, Lenck-Santini PP. Role of interictal epileptiform abnormalities in cognitive impairment. *Epilepsy Behav*. 2006;8:504-515.
7. Binnie CD. Cognitive impairment during epileptiform discharges: Is it ever justifiable to treat the EEG? *Lancet Neurol*. 2003;2:725-730.
8. Bjørnæs H, Bakke KA, Larsson PG, et al. Subclinical epileptiform activity in children with electrical status epilepticus during sleep: Effects on cognition and behavior before and after treatment with levetiracetam. *Epilepsy Behav*. 2013;27:40-48.
9. Henin S, Shankar A, Borges H, et al. Spatiotemporal dynamics between interictal epileptiform discharges and ripples during associative memory processing. *Brain*. 2021;144:1590-1602.
10. Larsson PG, Bakke KA, Bjørnæs H, et al. The effect of levetiracetam on focal nocturnal epileptiform activity during sleep – a placebo-controlled double-blind cross-over study. *Epilepsy Behav*. 2012;24:44-48.
11. Bal T, McCormick DA. What stops synchronized thalamocortical oscillations? *Neuron*. 1996;17:297-308.
12. Fernandez LMJ, Lüthi A. Sleep spindles: Mechanisms and functions. *Physiol Rev*. 2020;100:805-868.
13. Mak-McCully RA, Rolland M, Sargsyan A, et al. Coordination of cortical and thalamic activity during non-REM sleep in humans. *Nat Commun*. 2017;8:15499.
14. Schreiner T, Kaufmann E, Noachtar S, Mehrkens JH, Staudigl T. The human thalamus orchestrates neocortical oscillations during NREM sleep. *Nat Commun*. 2022;13:5231.
15. Steriade M, McCormick D, Sejnowski T. Thalamocortical oscillations in the sleeping and aroused brain. *Science*. 1993;262:679-685.
16. Hahn M, Joechner AK, Roell J, et al. Developmental changes of sleep spindles and their impact on sleep-dependent memory consolidation and general cognitive abilities: A longitudinal approach. *Dev Sci*. 2019;22:e12706.
17. Reynolds CM, Short MA, Gradisar M. Sleep spindles and cognitive performance across adolescence: A meta-analytic review. *J Adolesc*. 2018;66:55-70.
18. Denis D, Mylonas D, Poskanzer C, Bursal V, Payne JD, Stickgold R. Sleep spindles preferentially consolidate weakly encoded memories. *J Neurosci*. 2021;41:4088-4099.
19. Gais S, Mölle M, Helms K, Born J. Learning-dependent increases in sleep spindle density. *J Neurosci*. 2002;22:6830-6834.
20. Latchoumane CFV, Ngo HVV, Born J, Shin HS. Thalamic spindles promote memory formation during sleep through triple phase-locking of cortical, thalamic, and hippocampal rhythms. *Neuron*. 2017;95:424-435.e6.
21. Helfrich RF, Lendner JD, Mander BA, et al. Bidirectional prefrontal-hippocampal dynamics organize information transfer during sleep in humans. *Nat Commun*. 2019;10:3572.
22. Staresina BP, Bergmann TO, Bonnefond M, et al. Hierarchical nesting of slow oscillations, spindles and ripples in the human hippocampus during sleep. *Nat Neurosci*. 2015;18:1679-1686.
23. Steriade M. Grouping of brain rhythms in corticothalamic systems. *Neuroscience*. 2006;137:1087-1106.

24. Traub RD, Wong RK. Cellular mechanism of neuronal synchronization in epilepsy. *Science*. 1982;216:745-747.
25. Steriade M, Contreras D. Spike-wave complexes and fast components of cortically generated seizures. I. Role of neocortex and thalamus. *J Neurophysiol*. 1998;80:1439-1455.
26. Velasco M, Velasco F, Alcalá H, Dávila G, Díaz-de-León AE. Epileptiform EEG activity of the centromedian thalamic nuclei in children with intractable generalized seizures of the Lennox-Gastaut syndrome. *Epilepsia*. 1991;32:310-321.
27. Velasco M, Leon AED, Márquez I, et al. Temporo-spatial correlations between scalp and centromedian thalamic EEG activities of stage II slow wave sleep in patients with generalized seizures of the cryptogenic Lennox–Gastaut syndrome. *Clin Neurophysiol*. 2002;113:25-32.
28. Gadot R, Korst G, Shofty B, Gavvala JR, Sheth SA. Thalamic stereoelectroencephalography in epilepsy surgery: A scoping literature review. *J Neurosurg*. 2022;137:1210-1225.
29. Frauscher B, Bernasconi N, Caldairou B, et al. Interictal hippocampal spiking influences the occurrence of hippocampal sleep spindles. *Sleep*. 2015;38:1927-1933.
30. Klinzing JG, Tashiro L, Ruf S, Wolff M, Born J, Ngo HVV. Auditory stimulation during sleep suppresses spike activity in benign epilepsy with centrotemporal spikes. *Cell Rep Med*. 2021;2:100432.
31. Kramer MA, Stoyell SM, Chinappen D, et al. Focal sleep spindle deficits reveal focal thalamocortical dysfunction and predict cognitive deficits in sleep activated developmental epilepsy. *J Neurosci*. 2021;41:1816-1829.
32. McLaren JR, Luo Y, Kwon H, Shi W, Kramer MA, Chu CJ. Preliminary evidence of a relationship between sleep spindles and treatment response in epileptic encephalopathy. *Ann Clin Transl Neurol*. 2023;10:1513-1524.
33. Schiller K, Avigdor T, Abdallah C, et al. Focal epilepsy disrupts spindle structure and function. *Sci Rep*. 2022;12:11137.
34. Grigg-Damberger M, Gozal D, Marcus CL, et al. The visual scoring of sleep and arousal in infants and children. *J Clin Sleep Med*. 2007;03:201-240.
35. Iber C, Ancoli-Israel S, Chesson AL, Quan S. *The AASM manual for the scoring of sleep and associated events: Rules, terminology and technical specifications*. American Academy of Sleep Medicine; 2007.
36. Dahal P, Ghani N, Flinker A, et al. Interictal epileptiform discharges shape large-scale intercortical communication. *Brain*. 2019;142:3502-3513.
37. Gelinas JN, Khodagholy D, Thesen T, Devinsky O, Buzsáki G. Interictal epileptiform discharges induce hippocampal–cortical coupling in temporal lobe epilepsy. *Nat Med*. 2016;22:641-648.
38. Eden UT, Kramer MA. Drawing inferences from Fano factor calculations. *J Neurosci Methods*. 2010;190:149-152.
39. Kwon H, Walsh KG, Berja ED, et al. Sleep spindles in the healthy brain from birth through 18 years. *Sleep*. 2023;46:zsad017.
40. Mölle M, Born J. Chapter 7—Slow oscillations orchestrating fast oscillations and memory consolidation. In: Van Someren EJW, Van Der Werf YD, Roelfsema PR, Mansvelder HD, Lopes Da Silva FH, eds. *Progress in brain research. Vol. 193. Slow brain oscillations of sleep, resting state and vigilance*. Elsevier; 2011:93-110.
41. Truccolo W, Eden UT, Fellows MR, Donoghue JP, Brown EN. A point process framework for relating neural spiking activity to spiking history, neural ensemble, and extrinsic covariate effects. *J Neurophysiol*. 2005;93:1074-1089.
42. Frauscher B, von Ellenrieder N, Ferrari-Marinho T, Avoli M, Dubeau F, Gotman J. Facilitation of epileptic activity during sleep is mediated by high amplitude slow waves. *Brain J Neurol*. 2015;138(Pt 6):1629-1641.
43. Greene WH. *Econometric analysis*. Pearson Education; 2017.
44. Harrison MT, Amarasingham A, Kass E. Statistical identification of synchronous spiking. In: DiLorenzo, PM, Victor JD, eds. *Spike timing: Mechanisms and function*. CRC Press; 2013:42.
45. Bokil H, Andrews P, Kulkarni JE, Mehta S, Mitra PP. Chronux: A platform for analyzing neural signals. *J Neurosci Methods*. 2010; 192:146-151.
46. Nir Y, Staba RJ, Andrillon T, et al. Regional slow waves and spindles in human sleep. *Neuron*. 2011;70:153-169.
47. Cash SS, Halgren E, Dehghani N, et al. The human K-complex represents an isolated cortical down-state. *Science*. 2009;324:1084-1087.
48. Piper RJ, Richardson RM, Worrell G, et al. Towards network-guided neuromodulation for epilepsy. *Brain*. 2022;145:3347-3362.
49. Paz JT, Huguenard JR. Microcircuits and their interactions in epilepsy: Is the focus out of focus? *Nat Neurosci*. 2015;18:351-359.
50. Steriade M. Sleep, epilepsy and thalamic reticular inhibitory neurons. *Trends Neurosci*. 2005;28:317-324.
51. Spencer ER, Chinappen D, Emerton BC, et al. Source EEG reveals that Rolandic epilepsy is a regional epileptic encephalopathy. *NeuroImage Clin*. 2022;33:102956.
52. Eichenbaum H. Prefrontal–hippocampal interactions in episodic memory. *Nat Rev Neurosci*. 2017;18:547-558.
53. Lecci S, Fernandez LMJ, Weber FD, et al. Coordinated infraslow neural and cardiac oscillations mark fragility and offline periods in mammalian sleep. *Sci Adv*. 2017;3:e1602026.
54. Fogel SM, Smith CT. The function of the sleep spindle: A physiological index of intelligence and a mechanism for sleep-dependent memory consolidation. *Neurosci Biobehav Rev*. 2011; 35:1154-1165.
55. Hahn MA, Heib D, Schabus M, Hoedlmoser K, Helfrich RF. Slow oscillation-spindle coupling predicts enhanced memory formation from childhood to adolescence. *eLife*. 2020;9:e53730.
56. Dickey CW, Sargsyan A, Madsen JR, Eskandar EN, Cash SS, Halgren E. Travelling spindles create necessary conditions for spike-timing-dependent plasticity in humans. *Nat Commun*. 2021;12:1027.
57. Diba K, Buzsáki G. Forward and reverse hippocampal place-cell sequences during ripples. *Nat Neurosci*. 2007;10:1241-1242.
58. Bölsterli Heinzle BK, Fattinger S, Kurth S, et al. Spike wave location and density disturb sleep slow waves in patients with CSWS (continuous spike waves during sleep). *Epilepsia*. 2014;55:584-591.
59. van den Munckhof B, Gefferie SR, van Noort SAM, et al. Sleep slow-wave homeostasis and cognitive functioning in children with electrical status epilepticus in sleep. *Sleep*. 2020;43:zsaa088.
60. Kim U, Mccormick DA. Functional and ionic properties of a slow afterhyperpolarization in ferret perigeniculate neurons in vitro. *J Neurophysiol*. 1998;80:1222-1235.
61. Li Q, Westover MB, Zhang R, Chu CJ. Computational evidence for a competitive thalamocortical model of spikes and spindle activity in Rolandic epilepsy. *Front Comput Neurosci*. 2021;15:680549.
62. Steriade M. Spindling, incremental thalamocortical responses, and spike-wave epilepsy. In: Avoli M, Gloor P, Kostopoulos G, Naquet R, eds. *Generalized epilepsy: Neurobiological approaches*. Birkhäuser; 1990:161-180.